Mechanical resonance of quartz microfibers and boundary condition effects

Xinqi Chen, Sulin Zhang, Gregory J. Wagner,[a] Weiqiang Ding, and Rodney S. Ruoff[b]
Department of Mechanical Engineering, Northwestern University, Evanston, Illinois 60208

(Received 8 January 2004; accepted 18 February 2004)

We have measured the mechanical resonance of microscale quartz fibers to qualify the method of obtaining the Young's modulus of nanowires from their resonance frequency and geometry. An equation for a circular beam with a linearly varying cross-section is derived and used to calculate the resonance frequency shift. We have established a model to discuss the boundary condition effect on the resonance frequency. The Young's modulus of the quartz fibers has been determined by measuring the resonance frequency, and the geometry, and by applying the model that treats the influence of the type of clamp. The mean value from measurements of the fundamental resonance on 14 different microfibers is 70 ± 6 GPa. This mean value is close to 72 GPa, the Young's modulus of bulk fused quartz. Four resonance modes were observed in high vacuum and air. The mechanical resonance in high vacuum is linear at the fundamental vibration mode, and nonlinear for higher modes. © *2004 American Institute of Physics.* [DOI: 10.1063/1.1697635]

I. INTRODUCTION

Resonance vibration measurement offers a straightforward method for fitting the Young's modulus of nanostructures compared to tensile loading measurements. Carbon nanotubes have been resonantly excited at the fundamental frequency and higher harmonics and their elastic moduli were determined.[1–3] We have recently measured the resonance response of three amorphous SiO_x [$x\sim2$ by electron-energy-loss spectroscopy (EELS) characterization] nanowires and reported their mechanical properties,[4] while even smaller diameter amorphous SiO_x nanowires ($x\sim2$ by EELS characterization) were driven into resonance in a transmission electron microscope.[2] Both of these studies on the amorphous SiO_x nanowires[2,4] yielded anomolously low Young's modulus values relative to the fused silica (which is also amorphous) studied here. For example, the mean value for Young's modulus for the three SiO_x nanofibers whose resonance was fit in Ref. 4 was 47 GPa and for the five SiO_x nanofibers studied in Ref. 2 the mean value was 28 GPa. These values should be contrasted with the value of bulk fused quartz of 72 GPa. There is, therefore, the question of whether the mechanical resonance method is providing the correct value for the modulus of nanostructures. In part for this reason, we have chosen to study *microscale* quartz fibers as a way of qualifying the mechanical resonance method for obtaining Young's modulus values for the ever-growing class of newly synthesized nanoscale fibers, wires, and tubes. If there are ''problems'' associated with microscale samples, it is likely that the same sorts of issues will arise with nanoscale samples.

Quartz fiber finds wide applications in optical communications, and the mechanical properties of quartz fiber are also critical for its potential applications in microscale or nanoscale systems as a mechanical resonator and for structural applications such as in glass fiber reinforced composites. The tensile modulus of microscale quartz fibers is reported in Refs. 5 and 6, and the values vary from 56.3 to 72.3 GPa. The values reported in the literature are somewhat inconsistent, and the detailed experimental method used was, unfortunately, not well described. Here, we have measured the mechanical resonance at the fundamental and first overtone frequencies to fit the Young's modulus values of quartz fibers that we made with a glass puller in our laboratory.

II. EXPERIMENTS

The quartz fibers were made by pulling a 2-mm diameter fused quartz rod (GE Quartz, Inc., Ohio). Fourteen fibers with diameters varying from 20 to 130 μm and lengths varying from 4 to 30 mm were chosen for the measurements. They were bonded onto short copper wires (with diameter of 0.5 mm) with Elmer's glue (Ohio) for support.

The copper wires were then fixed onto a piezoelectric multilayer bender (Noliac A/S, Denmark, ceramic multilayer bender B1) for measurement of mechanical resonance. The copper wires and attached quartz fibers were aligned parallel to the piezoelectric multilayer bender to obtain the largest vibration amplitude. Most experiments were done under an optical microscope (10× to 40× Zoom Stereomicroscopes from Edmund Scientific, New Jersey), and the peak frequency was measured by observing the resonance by eye under the optical microscope. The fiber diameters were measured in a scanning electron microscope (LEO 1525 FE-SEM) and the fibers were rotated and imaged, which confirmed that they were round. The fiber length was measured under a wide stereomicroscope (Heerbrugg, Switzerland, Model WILD M32). To compare the mechanical resonance

[a]Current address: Sandia National Laboratories, MS 9402, Livermore, CA 94551.
[b]Author to whom correspondence should be addressed; electronic mail: r-ruoff@northwestern.edu

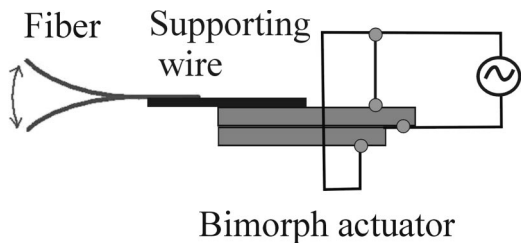

FIG. 1. Schematic drawing of the experimental setup. The supporting wire holding a microfiber is fixed at the end of the bender actuator.

in air versus vacuum, the resonance of the fibers was also measured in the SEM (at a pressure of 10^{-6}–10^{-7} Torr).

The schematic of the experimental setup is shown in Fig. 1. An ac electric field was applied to the piezoelectric bender actuator and the driving frequency was swept with a synthesized function generator (Stanford Research Systems, California, Model DS345). The oscillating bender plate excited the harmonic resonances of the microscale fibers.

III. RESULTS AND DISCUSSION

A. Realization of the first four harmonic resonances

For a singly-clamped uniform beam, the mechanical resonance frequency f_n for the nth mode is[7]

$$f_n=\frac{\beta_n^2}{2\pi}\sqrt{\frac{EI}{mL^4}}, \tag{1}$$

where E is the Young's modulus of the beam, I the cross-sectional area moment of the inertia, m the mass per unit length, L the beam length, and β_n the associated eigenvalue (the solution to $\cos\beta_n\cosh\beta_n=-1$). The first four modes have eigenvalues of $\beta_0=1.875$, $\beta_1=4.694$, $\beta_2=7.855$, and $\beta_3=10.996$.

Figure 2 shows the optical images of an oscillating microfiber. The first four harmonic resonance modes are excited and are shown in Figs. 2(a), 2(b), 2(c), and 2(d), respectively. The theoretical displacement of a uniform singly-clamped beam along the length L is[7]

$$\phi_n(x)=A_n[(\sin\beta_nL-\sinh\beta_nL)(\sin\beta_nx-\sinh\beta_nx)+(\cos\beta_nL+\cosh\beta_nL)(\cos\beta_nx-\cosh\beta_nx)], \tag{2}$$

where $\phi_n(x)$ is the displacement at point x of the beam for mode n and A_n is a normalization constant. The theoretical displacement curves for each mode are also plotted in Fig. 2. This result indicates that the node positions as predicted by Eq. (2) and as measured, are in close agreement.

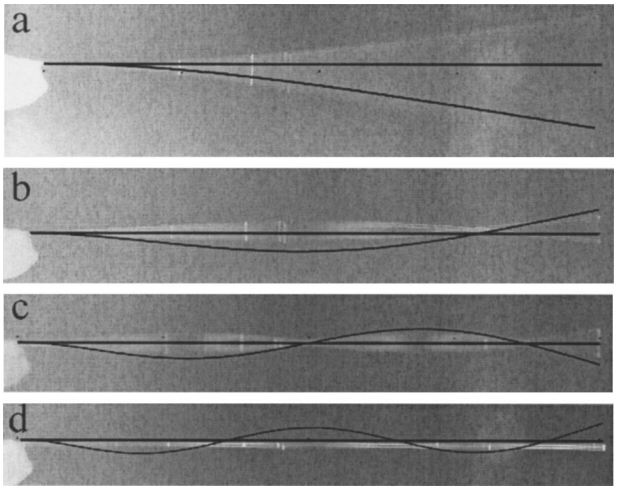

FIG. 2. Optical microscope pictures of an oscillating quartz microfiber. (a) The fundamental resonance, (b) the first overtone resonance, (c) the second overtone resonance, and (d) the third overtone resonance of the fiber. The insets are the theoretical displacement curves.

B. Effect of linear variation in cross section

One of the goals of these experiments is fitting the Young's modulus of the microscale (in diameter) quartz fibers according to Eq. (1). The quartz fibers were excited in air with the piezoelectric bender to find the resonance frequency at the fundamental and the first overtone. We find that the fundamental resonance could be observed easily; observation of the overtone resonance was found to depend on the ratio of the fiber length to the cross-section diameter. The variation of the cross-section diameter of the fibers along their length was measured and all fibers showed a linear variation, which we find to be typical for our pulled quartz fibers. The effect of this variation in cross section was taken into account by using a modified expression for the natural frequency based on a perturbation solution in the small parameter $\varepsilon=(D_1-D_0)/D_0$, where D_0 is the diameter at the fixed end of the vibrating fiber and D_1 is the diameter at the free end. The cross-sectional area and moment of inertia as functions of the length of the beam are then given, to the first order, by

$$A(x)=A_0[1+\varepsilon a(x)], \tag{3}$$

$$\frac{I(x)}{A(x)}=\frac{I_0}{A_0}[1+\varepsilon a(x)], \tag{4}$$

$$a(x)=2x/L, \tag{5}$$

where the subscript "0" indicates a quantity measured at the fixed end of the beam. The shift in frequency can then be computed according to (see Ref. 8 for details):

$$f_n=f_{n,0}(1+\varepsilon\nu_n), \tag{6}$$

$$\nu_n=\frac{1}{2L}\int_0^L\phi_n\left[\frac{L^4}{\beta_n^4}(2a''\phi_n''+4a'\phi_n''')+a\phi_n\right]dx. \tag{7}$$

In these expressions, $f_{n,0}$ is the natural frequency of mode n computed using the parameters measured at the fixed end. Primes on ϕ_n and a represent derivatives with respect to x. For a given mode, the integral in the expression for ν_n can be evaluated numerically. The results for the first few modes are (a) for the fundamental mode $\nu_0=-0.420$, (b) for the first overtone $\nu_1=0.218$, (c) for the second overtone $\nu_2=0.402$, and (d) for the third overtone $\nu_3=0.450$.

Note that for $D_1>D_0$, the shift in frequency is negative for the fundamental mode due to the increase of mass near

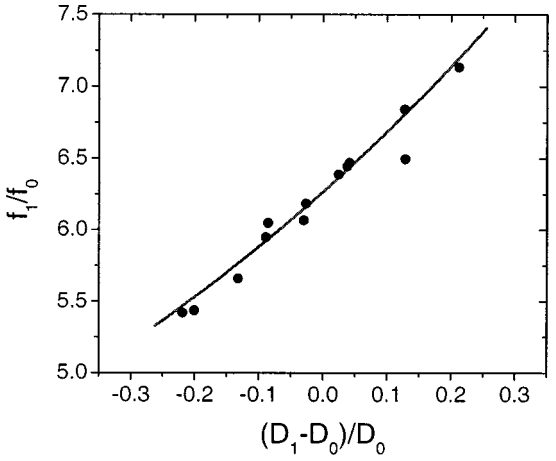

FIG. 3. The frequency ratio of the first overtone to the fundamental resonance vs the variation of the cross-sectional diameter. The solid line is the theoretical value and the dots are plotted based on the experimental data.

the end of the beam, but positive for the higher modes, for which increased stiffness dominates over the increased mass. Thus, if $D_0 > D_1$, the ratio of $f_1/f_0 < 6.267$, which is the theoretical value of the ratio for a uniform beam; if $D_0 < D_1$, then $f_1/f_0 > 6.267$. According to Eq. (6), we can see that the ratio is $f_1/f_0 = (f_{1,0}/f_{0,0})(1+0.218\varepsilon)/(1-0.420\varepsilon) = 6.267(1+0.218\varepsilon)/(1-0.420\varepsilon)$. Figure 3 shows the frequency ratio of the first overtone to the fundamental versus the variation of the cross-sectional diameter. The experimental values agree well with the analysis.

C. Boundary condition effects

In the previous section, the formula for the resonance frequency was based upon the assumption of perfect clamping. However, we do not achieve a perfectly rigid clamp in these experiments. We used Elmer's glue to attach the microfibers on the copper wires. Our tensile-loading experiments (DMA 2980 Dynamic Mechanical Analyzer, TA Instruments, Delaware) show that the Young's modulus of this glue is ~0.6 GPa, which means the clamp is much more compliant than the microfibers. Using the perfect-clamping assumption thus substantially underestimates the Young's modulus of the microfibers. In what follows, the clamping effect on the resonance frequency of the microfibers is taken into account by using a *beam-embedded-in-an-elastic-foundation* model.

Based on the energy conservation concept in a damping-free vibration, the fundamental angular frequency ω_0 ($\omega_0 = 2\pi f_0$) can be approximated by the following formula:[9]

$$\omega_0^2 = \frac{\int_L EI[y''(x)]^2 dx}{\int_L m[y(x)]^2 dx}, \tag{8}$$

where $y(x)$ is the deflection of the beam, and E, I, and m are the Young's modulus, the momentum of inertia, and unit mass of the beam, respectively. The integrations are evaluated along the length of the beam L.

To ensure the accuracy of the frequency using Eq. (8), the deflection function is chosen such that the boundary conditions are satisfied. In practice, the deflection function can be determined by considering the case in which the beam is subjected to a uniformly distributed unit force.

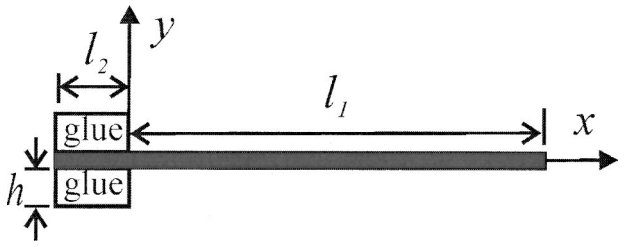

FIG. 4. Schematic drawing of the model of a beam-embedded-in-an-elastic foundation.

Figure 4 depicts the mechanics model in which the beam is embedded in an elastic foundation. Since only vibration in the plane of Fig. 4 is of interest, the clamping is simplified in the model by sandwiching the beam between glue layers. From the Euler–Bernoulli beam theory,[9] the governing equation for the beam deflection $y(x)$ under a uniformly distributed unit force along the beam is

$$\frac{d^4y(x)}{dx} + 4\lambda^4 H(x) y(x) = \frac{1}{EI}, \tag{9}$$

where $\lambda^4 = K/4EI$, K is the stiffness of the elastic foundation, and

$$H(x) = \begin{cases} 1 & x < 0 \\ 0 & x \geqslant 0 \end{cases}.$$

Using the boundary conditions for the free end at $x = l_1$, the deflection of the beam for the positive section can be written as

$$y_1(x) = \frac{1}{24EI}(l_1 - x)^4 + \alpha x + \beta, \quad (0 \leqslant x \leqslant l_1) \tag{10}$$

while for the negative section, the general solution to the deflection of the beam can be represented as

$$y_2(x) = Ae^{\lambda x}\sin\lambda x + Be^{\lambda x}\cos\lambda x + Ce^{-\lambda x}\cos\lambda x + De^{-\lambda x}\sin\lambda x + \frac{1}{K}, \quad (-l_2 \leqslant x \leqslant 0). \tag{11}$$

The six unknowns in Eqs. (10) and (11) can be determined by two boundary conditions at $x = -l_2$ and by compatibility conditions at $x = 0$. The compatibility conditions require that the deflection and the first three derivatives match between the solutions for the two segments

$$y_1(0) = y_2(0), \quad y_1'(0) = y_2'(0),$$
$$y_1''(0) = y_2''(0), \quad y_1'''(0) = y_2'''(0).$$

The boundary conditions at $x = -l_2$ must conform to the experiments. In the experiments, the left end of the fiber is embedded in the glue (it does not stick out of the glue clamp nor is it perfectly flush with the end of the glue deposit—it is in the interior of the glue deposit). Since the glue is compliant, the end ($x = -l_2$) of the fiber is neither perfectly clamped nor completely free, but constrained with a condition between these two limiting cases. By considering these two extreme conditions, the upper and lower limits of the frequency can be obtained. These two extreme conditions are

$$y_2(-l_2)=0, \quad y_2'(-l_2)=0, \quad \text{for a fixed end}$$

and

$$y_2''(-l_2)=0, \quad y_2'''(-l_2)=0, \quad \text{for a free end.}$$

The only undetermined variable in the above equations is the stiffness of the elastic foundation (the glue clamp) K, which is related to the Young's modulus E' and the geometry of the glue. To establish this relationship, only the embedded segment of the beam is considered in the following analysis.

Assume that the embedded segment of the beam undergoes a uniform downward displacement δ. The resultant force per unit length on the segment can be written as

$$F=F_{\text{top}}+F_{\text{bottom}}=\frac{2E'b\delta}{h}, \tag{12}$$

where b is the width of the glue layers, and h is the thickness of the glue layers, as seen in Fig. 1. On the other hand, if we regard the glue layer as a series of linear springs, one has

$$F=F_{\text{top}}+F_{\text{bottom}}=(K_{\text{top}}+K_{\text{bottom}})\,\delta=K\delta, \tag{13}$$

where the subscripts ''top'' and ''bottom'' denote the contributions from the top and bottom glue layers, respectively. Combining Eqs. (12) and (13), the stiffness of the glue foundation is

$$K=\frac{2E'b}{h}. \tag{14}$$

The fundamental angular frequency of the beam embedded in the glue at one end can thus be written as

$$\omega_0=\xi(K,l_2/l_1)\,\omega_0^{\text{PC}}(l_1) \tag{15}$$

where ξ is the correction factor that is a function of the stiffness of the glue foundation and the length of the section that is embedded into the glue, and $\omega_0^{\text{PC}}(l_1)$ is the fundamental angular frequency of the beam in the case of perfect clamping at $x=0$. In the limiting case of $K\to\infty$, $\xi(K,l_2/l_1)\to 1$, and ω_0 approaches $\omega_0^{\text{PC}}(l_1)$. If, on the other hand, $K\to 0$, and the point at $x=-l_2$ is perfectly clamped, $\xi(K,l_2/l_1)\to l_1^2(l_1+l_2)^2$, and ω_0 approaches to $\omega_0^{\text{PC}}(l_1+l_2)$. We used the geometry of one of the measured microfibers to estimate the correction factor, which is a function of the Young's modulus of the glue. The length and the diameter of the computed fiber are 8.93 mm and 23.30 μm, respectively. Based on our observation with both scanning electron and optical microscopy, the thickness of the glue layer is approximately 75 μm, l_2 is 1 mm, and the width of the glue layer is assumed to be the same as the fiber diameter. The plot was made based on the boundary condition of the fixed end case and is shown as Fig. 5. The correction factor approaches unity as the Young's modulus of the glue is increased. The solid line was plotted for the case where the fiber was attached by glue on each side (top and bottom) to solid foundations; the dashed line represents the case where the fiber is only attached by glue to a substrate beneath the microfiber. In the actual experiment, while the bottom glue layer is attached to a solid foundation, the glue on top of the microfiber, being only attached to the bottom glue layer, is more compliant and does not contribute significantly to the reinforcement of the clamp. Thus the experimental conditions are intermediate between the two plotted limiting cases in Fig. 5. For the glue with Young's modulus of 0.6 GPa, the difference between the two limiting cases is just 0.3%. To simplify the treatment, we chose the first case to calculate the correction factors for our microfibers.

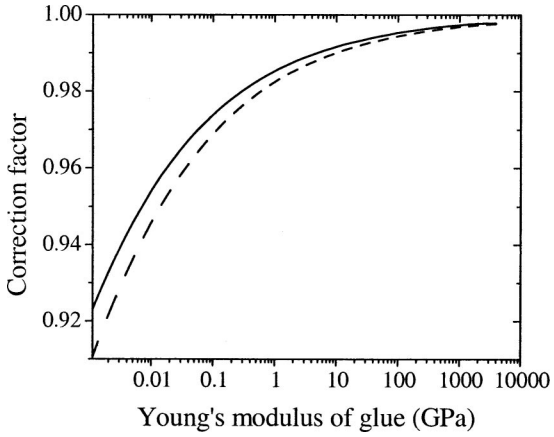

FIG. 5. The correction factor as a function of the Young's modulus of the clamp. The solid line was plotted for the case where the fiber was attached by glue on each side (top and bottom) to solid foundations; the dashed line represents the case where the fiber is only attached by glue to a substrate beneath the microfiber.

In many resonance experiments, the nanowires that are driven into resonance were simply attached onto a substrate on one end without any intentional clamp. In such cases, the relatively weak van der Waals force and any adhesive force that may be present, are the only force acting between the nanowire and the substrate. The above derivation is applicable for this case except that the stiffness of the foundation needs to be computed. (This case will be discussed in a separate article.)

It should be mentioned that the analysis presented above is valid for beams with a uniform cross-section. The solution to the deflection function is very tedious if a linearly varying cross-section is considered. Decoupling these two effects is possible here since the cross-section diameter varied slowly with the length of the microfibers.

D. Fit Young's modulus

Fourteen microfibers have been mechanically excited and Table I shows the geometry of these fibers and their resonance frequency. The shifts of the resonance frequency caused by cross-sectional linear variation were estimated based on Eq. (6). The correction factors caused by the compliant clamp were estimated according to Eq. (15). The fixed end boundary condition was used for this computation. (The correction factors based on the two limiting boundary conditions discussed above are very close, because of the long embedded section.) The values of the Young's modulus have been fit according to Eq. (1). The density of the quartz fibers is assumed to be 2.2 g/cm^3, which is based on data for the 2 mm fused quartz rod from which they were fabricated by pulling. E_0 is the Young's modulus calculated from the fundamental resonance frequency. The mean value for the Young's modulus of 14 quartz microfibers determined from

TABLE I. Young's modulus of quartz fiber measured with resonance method.[a]

Number	L (mm) ($\pm$0.01)	D_0 (μm) ($\pm$0.01)	D_1 (μm) ($\pm$0.01)	f_0 (Hz) ($\pm$1)	f_1 (Hz) ($\pm$1)	f_1/f_0	Factor 1	Factor 2	E_0 (GPa)
1	8.93	23.30	18.20	249	1349	5.42	1.09	0.983	70.8$\pm$0.6
2	8.22	31.94	25.53	397	2158	5.44	1.08	0.977	71.0$\pm$0.5
3	7.18	32.28	33.50	461	2971	6.44	0.984	0.973	66.4$\pm$0.4
4	3.92	36.06	32.86	1733	10307	5.95	1.04	0.948	63.3$\pm$0.6
5	7.71	38.14	34.89	490	2964	6.05	1.04	0.972	64.7$\pm$0.4
6	6.79	36.24	35.28	571	3531	6.18	1.01	0.970	61.6$\pm$0.4
7	7.61	41.42	35.95	537	3039	5.66	1.06	0.970	60.4$\pm$0.4
8	5.53	45.88	51.74	997	6821	6.84	0.946	0.956	60.6$\pm$0.4
9	6.35	56.70	68.74	987	7042	7.13	0.911	0.955	73.1$\pm$0.4
10	9.58	62.46	70.50	504	3274	6.50	0.946	0.968	73.4$\pm$0.4
11	6.53	73.95	77.00	1274	8243	6.47	0.983	0.947	70.0$\pm$0.4
12	5.70	103.3	103.4	2451	⋯	⋯	1.000	0.925	78.1$\pm$0.5
13	37.8	123	126	72	460	6.39	0.990	0.986	80.6$\pm$0.4
14	30.4	133	129	119	722	6.07	1.01	0.982	78.1$\pm$0.4

[a]L: length; D_0: diameter at the fixed end; D_1: free end diameter; f_0: fundamental resonance frequency; f_1: first overtone resonance frequency; Factor 1: correction factor based on the treatment of linear variation of the cross-section of the fibers; Factor 2: correction factor based on the treatment of the model of a beam-embedded-in-an-elastic foundation.

the fundamental resonance is 70 GPa, reasonably close to the Young's modulus 72 GPa of the precursor 2-mm diameter bulk fused quartz.[10] The result suggests that resonance vibration may be a reasonable method to use to obtain the mechanical properties of microfibers if sufficient care is taken in the treatments of the boundary condition(s) and a large number of specimens are measured. It also suggests that a relatively large number of samples need to be measured to achieve a mean value that one might trust as being meaningful.

E. Comparison of vibration in air and vacuum

Vibration amplitude and frequency at the fundamental mode for a quartz microfiber mounted at different orientations with respect to the bender plate was also studied. The quartz fiber orientation was varied from parallel to perpendicular. The vibration amplitude is a maximum when the fiber is parallel to the bender actuator and decreases monotonically reaching a minimum value when it is perpendicular to the bender actuator. The change of the vibration amplitude is attributed to the variation of the perpendicular driving force component on the fiber. The perpendicular driving force component is a maximum when the fiber is parallel to the bender and a minimum when it is perpendicular to the bender. It is known that tensile or compressive force on a beam can affect its resonance frequency,[8] so that if there is some force component along the fiber length, its resonance frequency may shift from its true resonance. We note that the frequency shift was negligible for measurement of the same microfiber oriented parallel, and also 30, 60, and 90° off parallel. However, the amplitude varied from A_0 (for parallel) to 0.87, 0.78, and $0.60\times A_0$ for 30, 60, and 90° off parallel, respectively.

We also compared the mechanical resonance of the same microfiber in a scanning electron microscopy vacuum chamber and in air, shown in Fig. 6. The results indicate that the resonance frequency of the principal peak is essentially the same, but the quality factor of the resonance is significantly different. The quality factor Q of the fundamental resonance in vacuum was $\sim$2000; in air there was a large damping and Q was only 25.

A second mechanical resonance for the natural resonance was detected in vacuum. This is an out-of-plane vibration. The small difference in values for the natural frequency is probably caused by a slight geometric asymmetry of the cross section of the quartz fiber at the free end. In Fig. 6, the triangles indicate increasing driving frequency and the circles indicate decreasing driving frequency. For the fundamental resonance, the two curves match closely. For overtones, they evidently match well in air because of the huge damping effect; however in vacuum, a nonlinear effect was observed and the curves show hysteresis. As the driving frequency is increased from below, the response amplitude

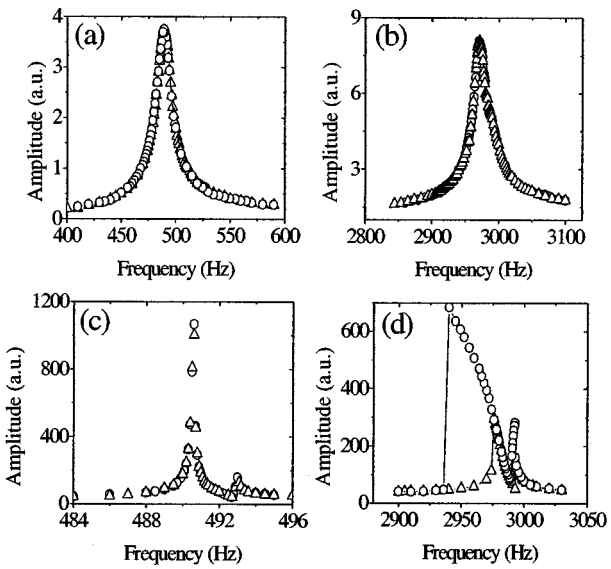

FIG. 6. (a) The fundamental and (b) first overtone vibration amplitude vs the driving frequency in air of a quartz microfiber; (c) and (d) show the vibration amplitude vs the driving frequency curve of the first two modes in high vacuum (triangle: frequency increasing; circle: frequency decreasing).

reaches a maximum and then decreases; as the driving frequency decreases from above, the response amplitude increases until a higher point is reached. At that frequency, the amplitude jumps to a lower value. This softening behavior results from the effect of the beam momentum in the axial direction. The axial force is developed by the transverse deflection of the fiber. The effect might be negligible for small amplitude motion. However, it results in this nonlinear effect when the amplitude is large. For the doubly clamped beam, the axial force will bend the amplitude-frequency curve to the right when the amplitude of the vibration is greater than the critical point.[11] This has been known as the ''hard-spring effect.'' The axial force has a more significant effect on the overtones than on the fundamental, since the ratio of axial to transverse motion is larger for the overtones (see Ref. 12 for a detailed mathematical treatment).

IV. CONCLUSIONS

We have investigated the mechanical resonance of quartz microfibers pulled from a quartz rod. A best-fit equation for a circular beam with linearly varying cross-sectional diameter was derived and used to calculate the resonance frequency shift. An analytical model, in which the effects of nonrigid clamping conditions on the natural resonance frequency are taken into account, was developed. The Young's modulus of each of the quartz fibers has been determined by measuring the natural resonance frequency; the mean value from measurements on 14 different microfibers is 70 ± 6 GPa which can be compared to that of bulk fused quartz, 72 GPa. The Young's modulus that is fit to the resonance data does not vary significantly with geometry, and the behavior seems in every way to be well described by engineering beam theory, so one may be confident that the true Young's modulus of the material is being determined. The mechanical resonance of a quartz fiber in air ($Q=25$) is strongly damped compared to vacuum ($Q=2000$) and this damping masks nonlinear effects, including a hysteretic response present in the overtone resonance excited in vacuum.

ACKNOWLEDGMENTS

We gratefully acknowledge the Office of Naval Research *Mechanics of Nanostructures* grant (Award No. N000140210870), and the NASA University Research, Engineering and Technology Institute on Bio Inspired Materials (BIMat) under Award No. NCC-1-02037. We thank H. Riecke for an insightful suggestion regarding the mathematical derivations and A. L. Ruoff for discussions regarding the compliant clamp.

APPENDIX

In the calculations of the unknown coefficients in Eqs. (10) and (11), careful treatment must be introduced to avoid roundoff errors. Here, all the unknowns are represented by a Taylor-series expansion

$$\xi=\xi_0+\xi_1\varepsilon+o(\varepsilon^2), \tag{A1}$$

where ξ stands for the unknowns, and $\varepsilon=e^{-2\lambda l_2}$ is a small number based on the experimental setup; ξ_0, ξ_1 are the zeroth and first-order terms of ξ, respectively. In our simulation, the second- and higher-order terms are ignored. Accordingly, the numerical error is on the order of $o(\varepsilon^2)$. For the calculation of α and β, we used the following formula:

$$\frac{1}{a_0+a_1\varepsilon}\approx\frac{1}{a_0}\left(1-\frac{a_1}{a_0}\varepsilon\right), \quad (a_0\neq 0). \tag{A2}$$

Once the unknowns are obtained, the integrations in Eq. (8) were calculated in a similar way, i.e., by splitting each of the integrations into two terms: the zeroth- and first-order terms, which were then separately calculated.

[1] P. Poncharal, Z. L. Wang, D. Ugarte, and W. A. de Heer, Science **283**, 1513 (1999).
[2] Z. L. Wang, R. P. Gao, P. Poncharal, W. A. de Heer, Z. R. Dai, and Z. W. Pan, Mater. Sci. Eng., C **16**, 3 (2001).
[3] Ruiping Gao, Zhong L. Wang, Zhigang Bai, Walter A. de Heer, Liming Dai, and Mei Gao, Phys. Rev. Lett. **85**, 622 (2000).
[4] D. A. Dikin, X. Chen, W. Ding, G. Wagner, and R. S. Ruoff, J. Appl. Phys. **93**, 226 (2003).
[5] D. J. Fisher, *Mechanical and Corrosion Properties: Nonmetal* (Trans Tech, Massachusetts, 1980), p. 84.
[6] *Engineered Materials Handbook, Vol. 1, Composites, Materials* (ASM International, Ohio), p. 360.
[7] L. Meirovich, *Elements of Vibration Analysis* (McGraw-Hill, New York, 1975), p. 212.
[8] P. M. Morse, *Vibration and Sound* (McGraw-Hill, New York, 1948), pp. 164 and 116.
[9] S. Timoshenko, D. H. Young, and W. Weaver, Jr., *Vibration Problems in Engineering*, 4th ed. (Wiley, New York, 1974), p. 464.
[10] The data of the mechanical properties of fused quartz were supplied by GE Quartz, Inc., Ohio. The data is available on http://www.gequartz.com/en/mech.htm.
[11] H. A. C. Tilmans, M. Elwenspoek, and J. H. J. Fkuitman, Sens. Actuators, A **30**, 35 (1992).
[12] E. C. Haight and W. W. King, J. Acoust. Soc. Am. **52**, 899 (1972).